Journal of Inorganic and Organometallic Polymers and Materials (2020) 30:417–426
https://doi.org/10.1007/s10904-019-01200-5

Thermodynamic and Thermal Properties of Solvation for Nano Nickel Ferrite and Nano Zinc Ferrite Prepared by the Sol–Gel Method in Different CH_3COOH Concentrations at Different Temperatures

M. A. Mousa[1] · E. A Gomaa[2] · M. Khairy[1,3] · M. E. Eltanany[1]

Received: 13 April 2019 / Accepted: 19 May 2019 / Published online: 30 May 2019

Abstract

The solubility of nickel ferrite and zinc ferrite in an aqueous solution of acetic acid was studied gravimmetrically by varying the concentration of acetic acid at different temperatures ranging from 25 to 45 °C. The molar solubility and thermodynamic parameters of nano nickel and nano zinc ferrites have been evaluated. In this work, we observed how the concentration of CH_3COOH and temperature affected the solubility of nano nickel and nano zinc ferrites at temperatures of 298, 303, 308, 313, 318 K. The two ferrites were prepared by sol–gel method. Structure and particle size of the reaction products were determined by X-ray diffraction and TEM analysis. It was found that the two ferrites were pure powder of $NiFe_2O_4$ and $ZnFe_2O_4$ with a cubic structure with mean particle size 21 and 30 nm respectively. The solubility of the two ferrites in different solutions of CH_3COOH was measured gravimmetrically by the evaporation process using I.R. Lamp. It was found that the solubility increased with an increasing mole fraction of different CH_3COOH solutions and increased also with increasing of temperature due to more solvation process. All solvation parameters were discussed. We need to mix the two nano ferrites in a safe solvent for different cancer chemotherapy treatment. The aim of the work is to dissolve the very insoluble nano nickel and nano zinc ferrites in weak acid like acetic acid,which is used in hyperthermia and also kill cancer tumors. Also the uses of nano ferrites as magnetic fluid hyperthermia agents and good carriers for chemotherapeutic agent. The aim of this work is to dissolve the very insoluble nano nickel and nano zinc ferrites prepared by sol–gel in CH_3COOH at different concentrations, then we can neutralize the excess acid. The target of this work is to increase the solubility of both nano nickel and nano zinc ferrites with increasing temperature. The aim also in this work is to give the helpful nickel nano ferrite data necessary for hyperthermia and killing cancer tumors, especially in the skin.

Keywords Molar solubility · Nickel ferrite · Zinc ferrite · Molar ratio · Effect of temperature · Solvation processes

1 Introduction

Nanomaterials are substances which are prepared from its bulk materials and used at a tiny scale. They measure from (1–100) nm. They may be in the form of particles, tubes, rods or fibers. They have a large surface area. The nanomaterials differ from its bulk materials in physical properties and behave differently if they enter the body. There are different methods for preparing nanomaterials which can be divided into two main classes i.e. (a) bottom-up approach and (b) top-down approach [1] the two approaches contain different methods for preparations such as, solid-state method [2], co-precipitation [3–6], citrate processes [4], autoclave (hydrothermal treatment), thermal decomposition or (combustion) method, citrate processes [4], sol–gel method [5], electrochemical [6, 7] and wet high energy ball milling [8]. In the

Electronic supplementary material The online version of this article (https://doi.org/10.1007/s10904-019-01200-5) contains supplementary material, which is available to authorized users.

✉ E. A Gomaa
aa.sh_04@yahoo.com

[1] Chemistry Department, Faculty of Science, Benha University, Benha, Egypt

[2] Chemistry Department, Faculty of Science, Mansoura University, Mansoura 35516, Egypt

[3] Chemistry Department, College of Science, Imam Mohammed Ibn Saud Islamic University, Riyadh, Saudi Arabia

present work nickel ferrite and zinc ferrite were synthesized by the sol–gel method. The solubility of ferrites as nanomaterials in mixed solvents has great importance in many medicinal and industrial processes such as in laboratory uses and a lot of manufacturing. Nickel ferrite [$NiFe_2O_4$] and zinc ferrite ($ZnFe_2O_4$) nanoparticles are attracted in recent days due to their high magnetic permeability, non-toxicity, low eddy current loss, excellent phase stability, high electronic conductivity and their low cost [9]. Nickel ferrite ($NiFe_2O_4$) finds numerous technological applications, such as gas sensor [10, 11], magnetic fluids [12], catalysts [13–15], photomagnetic materials [16] and microwave devices [17]. Zinc ferrite ($ZnFe_2O_4$) has more specific applications, including as a promising semiconductor photocatalyst [18, 19], photoinduced electron transfer [20], photoelectrochemical cells [21] and photochemical hydrogen production [22, 23]. The aim of the work is to dissolve the very insoluble nano nickel ferrite and nano zinc ferrite in weak acid like acetic acid. The target is to increase the solubilities of nano nickel ferrite and nano zinc ferrite with increasing temperature. Giving data which help the use of the selected nano ferrites given here in this work in hyperthermia and also kill cancer tumors. The two ferrites used are magnetic fluid and good carriers for chemotherapeutic agent and can the acid be neutralized. Also our aim is to give valuable data necessary for using nano zinc and nano nickel ferrites in the industry, especially for producing new colors and as electrodes in batteries.

2 Experimental

2.1 Materials

Nickel nitrate hexahydrate [$Ni(NO_3)_2{\cdot}6H_2O$], zinc nitrate hexahydrate [$Zn(NO_3)_2{\cdot}6H_2O$] and ferric (lll) nitrate [$Fe(NO_3)_3{\cdot}9H_2O$] were acquired from Oxford Laboratory, Mumbai. Citric acid ($C_6H_8O_7{\cdot}H_2O$) was purchased from VEB Berlin. Chemie. CTAB (98%) was purchased from Aldrich. Acetic acid glacial was purchased from Adwic. Double distilled water was used throughout all the experiments.

2.2 Synthesis of Nano Nickel Ferrite by Sol–Gel Method

4.2666 g of citric acid ($C_6H_8O_7{\cdot}H_2O$) and 0.02 g of CTAB were dissolved into 100 ml of distilled water with stirring at room temperature. Also, a complete dissolving of 2.91 g of nickel nitrate [$Ni(NO_3)_2{\cdot}6H_2O$] and 8.08 g of ferric nitrate [$Fe(NO_3)_3{\cdot}9H_2O$] into 100 ml distilled water with stirring at room temperature. Then, a continuous stirring for the mixture for 4 h at 90 °C. Then, heated at 180 °C in a drying oven. Pure nickel ferrite gel was obtained and was calcined at 400 °C for 2 h. The molar ratio of Ni^{2+} to Fe^{3+} was 1:2 [4].

2.3 Synthesis of Nano Zinc Ferrite by Sol–Gel Method

4.2666 g of citric acid ($C_6H_8O_7{\cdot}H_2O$) and 0.02 g of CTAB were dissolved into 100 ml of distilled water with stirring at room temperature. Also, a complete dissolving of 2.97 g of zinc nitrate [$Zn(NO_3)_2{\cdot}6H_2O$] and 8.08 g of ferric nitrate [$Fe(NO_3)_3{\cdot}9H_2O$] into 100 ml distilled water with stirring at room temperature. Then, a continuous stirring for the mixture for 4 h at 90 °C. Then, heated at 180 °C in a drying oven. Pure zinc ferrite gel was obtained and was calcined at 400 °C for 2 h. The molar ratio of Zn^{2+} to Fe^{3+} was 1:2 [4].

2.4 Preparation of Saturated Solutions and Solubility Measurements

Saturated solutions of nano nickel ferrite and nano zinc ferrite were prepared by dissolving solid amount in closed test tubes containing different aqueous concentrations of acetic acid. Then, tubes were put in water thermostat for a period of three days at different temperatures of 298, 303, 308, 313, 318 K [24–30] till equilibrium reached. Solubility of nano nickel ferrite and nano zinc ferrite in each mixture was measured by taking 1 ml of each saturated solution putting in a small weighed beaker (10 ml) and evaporate under I.R. lamp till dryness and then reweight [30–32].

3 Results and Discussion

3.1 X-ray Analysis for $NiFe_2O_4$ and $ZnFe_2O_4$

As shown in Fig. 1a XRD of $NiFe_2O_4$ shows diffraction peaks at 2θ = 30.448, 35.793, 43.531, 57.499, 63.208, 71.738, and 74.694, which refer to (111), (220), (311), (400), (422), (511), (440), (620) (JCPDS no. 10-325) [33, 34]. There is no such a side peaks, which confirms preparation of the pure spinel cubic structure of $NiFe_2O_4$.

Figure 1b shows the XRD pattern of $ZnFe_2O_4$ with diffraction peaks 2θ = 30.1, 35.2, 42.9, 53.2, 56.50, and 63.2, which corresponds to (220), (311), (400), (422), (511), and (400) (JCPDS no. 22–1012) without any presensce of side products peaks or reactants [35], which confirms preparation of the pure spinel cubic structure of $ZnFe_2O_4$. By using Sherrer's equation for calculating the crystalline size [34].

$$L = \frac{k\lambda}{\beta \cos\theta} \quad (1)$$

where L is the average crystalline size derived XRD pattern, k is sphere shape factor, λ is the wavelength of the used

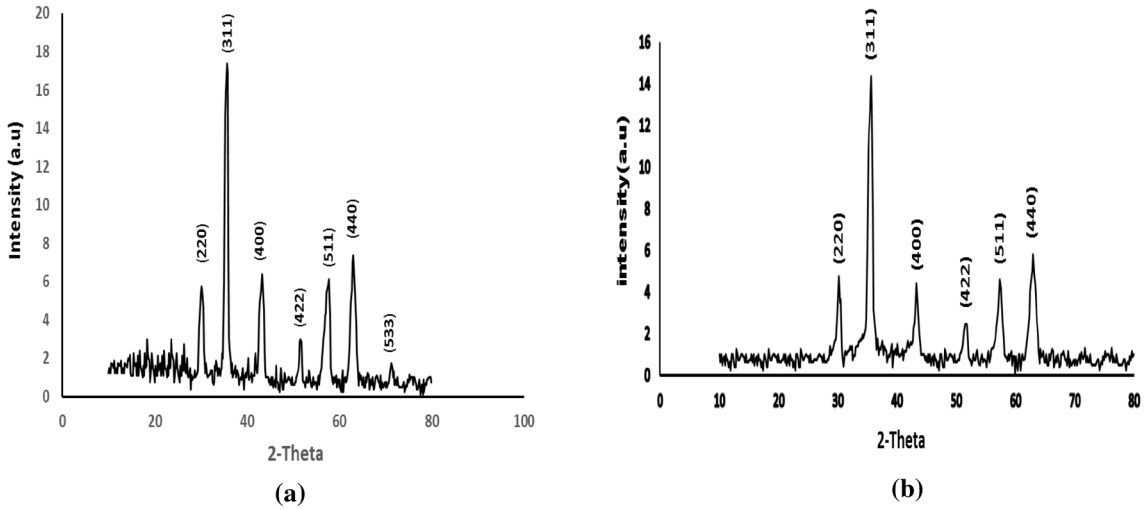

Fig. 1 XRD patterns of **a** $NiFe_2O_4$ and **b** $ZnFe_2O_4$

source, θ is the angle of diffraction, and (β) is (FWHM). The results of the average crystallite size was 21 nm for $NiFe_2O_4$, and 30.7 for $ZnFe_2O_4$.

3.2 TEM

TEM morphologies of the prepared $NiFe_2O_4$, and $ZnFe_2O_4$ nanoparticles are presented in Fig. 2. $NiFe_2O_4$, and $ZnFe_2O_4$ powders as synthesized by sol–gel process exhibit a network with voids and pores formed by the escaping gases during the combustion reaction. This type of porous network is typical of combustion synthesized powders. Heating has resulted in sintering of the well-faceted grains to form porous solid bodies, where the porosity is caused by the evaporation of gases during the synthesis process.

3.3 Thermodynamic Solvation Parameters

3.3.1 Molar Solubility

The molar solubility of $NiFe_2O_4$ and $ZnFe_2O_4$ nanoparticles in different concentration of aqueous acetic acid was calculated according to Eq. (2) [35].

$$\text{Molar solubility (S)} = (W \times 1000)/(\text{M.wt}) \quad (2)$$

where W is the weight of 1 ml of the saturated solution after the evaporation process in the small cups using I.R. lamp and M.wt is the molecular weight of nickel ferrite and zinc ferrite and the data obtained are tabulated in Tables 1, 2, 3, 4, 5, 6, 7, 8, 9, 10.

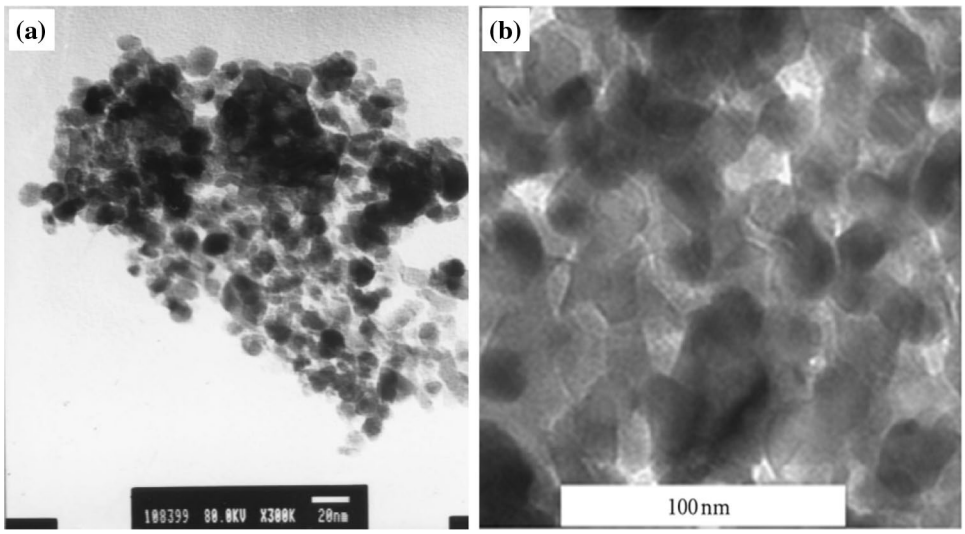

Fig. 2 TEM images for **a** $NiFe_2O_4$ and **b** $ZnFe_2O_4$

Table 1 Solubility S, Log solubility, log activity coefficient (logγ), solubility product (pKsp), Gibbs free energy (ΔG) and transfer Gibbs free enery (ΔG_t) for nano nickel ferrite prepared by sol–gel method at different mole fraction (Xs), different concentrations of CH_3·COOH at 298 K

Xs (CH_3·COOH)	S	Log S	log $\gamma_{\pm}$	pKsp	ΔG (J/mol)	ΔG_t (kJ/mol)
0.062	0.0026	− 2.5918	− 0.0256	2.5918	14,789.2047	0
0.143	0.0035	− 2.4685	− 0.0299	2.4585	14,028.9061	− 0.7603
0.255	0.0049	− 2.3360	− 0.0356	2.3060	13,158.4257	− 1.6308
0.417	0.0073	− 2.2056	− 0.0433	2.1356	12,186.0398	− 2.6032

Table 2 Solubility S, Log solubility, log activity coefficient (logγ), solubility product (pKsp), Gibbs free energy (ΔG) and transfer Gibbs free enery (ΔG_t) for nano nickel ferrite prepared by sol–gel method at different mole fraction (Xs), different concentrations of CH_3·COOH at 303 K

Xs (CH_3·COOH)	S	Log S	log $\gamma_{\pm}$	pKsp	ΔG (J/mol)	ΔG_t (kJ/mol)
0.062	0.0030	− 2.5248	− 0.0277	2.5248	14,648.9262	0
0.143	0.0042	− 2.3781	− 0.0328	2.3781	13,797.2984	− 0.8516
0.255	0.0058	− 2.2331	− 0.0387	2.2331	12,956.3466	− 1.6926
0.417	0.0090	− 2.0477	− 0.0479	2.0477	11,880.7100	− 2.7682

Table 3 Solubility S, Log solubility, log activity coefficient (logγ), solubility product (pKsp), Gibbs free energy (ΔG) and transfer Gibbs free energy (ΔG_t) for nano nickel ferrite prepared by sol–gel method at different mole fraction (Xs), different concentrations of CH_3·COOH at 308 K

Xs (CH_3·COOH)	S	Log S	log $\gamma_{\pm}$	pKsp	ΔG (J/mol)	ΔG_t (kJ/mol)
0.062	0.0035	− 2.4569	− 0.0299	2.4569	14,489.6647	0
0.143	0.0047	− 2.3260	− 0.0348	2.3260	13,717.9367	− 0.7717
0.255	0.0068	− 2.1653	− 0.0419	2.1653	12,769.9001	− 1.7198
0.417	0.0104	− 1.9820	− 0.0517	1.9820	11,689.1633	− 2.8005

Table 4 Solubility S, Log solubility, log activity coefficient (logγ), solubility product (pKsp), Gibbs free energy (ΔG) and transfer Gibbs free energy (ΔG_t) for nano nickel ferrite prepared by sol–gel method at different mole fraction (Xs), different concentrations of CH_3·COOH at 313 K

Xs (CH_3·COOH)	S	Log S	log $\gamma_{\pm}$	pKsp	ΔG (J/mol)	ΔG_t (kJ/mol)
0.062	0.0042	− 2.3771	− 0.0328	2.3771	14,246.9298	0
0.143	0.0056	− 2.2495	− 0.0380	2.2495	13,482.2151	− 0.7647
0.255	0.0077	− 2.1123	− 0.0445	2.1123	12,659.8957	− 1.5870
0.417	0.0113	− 1.9451	− 0.0539	1.9451	11,657.8039	− 2.5891

Table 5 Solubility S, Log solubility, log activity coefficient (logγ), solubility product (pKsp), Gibbs free energy (ΔG) and transfer Gibbs free enery (ΔG_t) for nano nickel ferrite prepared by sol–gel method at different mole fraction (Xs), different concentrations of CH_3·COOH at 318 K

Xs (CH_3·COOH)	S	Log S	log $\gamma_{\pm}$	pKsp	ΔG (J/mol)	ΔG_t (kJ/mol)
0.062	0.0051	− 2.2960	− 0.0360	2.2960	13,980.6502	0.0000
0.143	0.0067	− 2.1758	− 0.0413	2.1758	13,248.8782	− 0.7318
0.255	0.0088	− 2.0572	− 0.0474	2.0572	12,526.7280	− 1.4539
0.417	0.0124	− 1.9050	− 0.0565	1.9050	11,599.6150	− 2.3810

Table 6 Solubility S, Log solubility, log activity coefficient (logγ), solubility product (pKsp), Gibbs free energy (ΔG) and transfer Gibbs free energy (ΔG_t) for nano zinc ferrite prepared by sol–gel method at different mole fraction (Xs), different concentrations of CH_3·COOH at 298 K

Xs (CH_3·COOH)	S	Log S	log $\gamma_{\pm}$	pKsp	ΔG (J/mol)	ΔG_t (kJ/mol)
0.062	0.0035	− 2.4522	− 0.0301	2.4522	13,992.4294	0
0.143	0.0044	− 2.3608	− 0.0334	2.3608	13,470.9270	− 0.5215
0.255	0.0055	− 2.2561	− 0.0377	2.2561	12,873.4989	− 1.1189
0.417	0.0071	− 2.1517	− 0.0425	2.1517	12,278.0161	− 1.7144

Table 7 Solubility S, Log solubility, log activity coefficient (logγ), solubility product (pKsp), Gibbs free energy (ΔG) and transfer Gibbs free enery (ΔG_t) for nano zinc ferrite prepared by sol–gel method at different mole fraction (Xs), different concentrations of CH_3·COOH in CH_3·COOH–H_2O mixtures at 303 K

Xs (CH_3·COOH)	S	Log S	log $\gamma_{\pm}$	pKsp	ΔG (J/mol)	ΔG_t (kJ/mol)
0.062	0.0044	− 2.3579	− 0.0335	2.3579	13,680.4148	0
0.143	0.0054	− 2.2682	− 0.0372	2.2682	13,159.9783	− 0.5204
0.255	0.0068	− 2.1669	− 0.0418	2.1669	12,572.0754	− 1.1083
0.417	0.0086	− 2.0634	− 0.0471	2.0634	11,971.6870	− 1.7087

Table 8 Solubility S, Log solubility, log activity coefficient (logγ), solubility product (pKsp), Gibbs free energy (ΔG) and transfer Gibbs free enery (ΔG_t) for nano zinc ferrite prepared by sol–gel method at different mole fraction (Xs), different concentrations of CH_3·COOH at 308 K

Xs (CH_3·COOH)	S	Log S	log $\gamma_{\pm}$	pKsp	ΔG (J/mol)	ΔG_t (kJ/mol)
0.062	0.0053	− 2.2761	− 0.0368	2.2761	13,423.4486	0
0.143	0.0065	− 2.1900	− 0.0407	2.1900	12,916.0809	− 0.5074
0.255	0.0082	− 2.0849	− 0.0459	2.0849	12,296.2415	− 1.1272
0.417	0.0105	− 1.9797	− 0.0518	1.9797	11,675.7883	− 1.7477

Table 9 Solubility S, Log solubility, log activity coefficient (logγ), solubility product (pKsp), Gibbs free energy (ΔG) and transfer Gibbs free energy (ΔG_t) for nano zinc ferrite prepared by sol–gel method at different mole fraction (Xs), different concentrations of CH_3·COOH at 313 K

Xs (CH_3·COOH)	S	Log S	log $\gamma_{\pm}$	pKsp	ΔG (J/mol)	ΔG_t (kJ/mol)
0.062	0.0062	− 2.2063	− 0.0399	2.2063	13,223.4806	0
0.143	0.0075	− 2.1230	− 0.0439	2.1230	12,723.6794	−0.4998
0.255	0.0095	− 2.0239	− 0.0492	2.0239	12,129.8238	− 1.0937
0.417	0.0120	− 1.9220	− 0.0554	1.9220	11,519.1507	− 1.7043

Table 10 Solubility S, Log solubility, log activity coefficient (logγ), solubility product (pKsp), Gibbs free energy (ΔG) and transfer Gibbs free enery (ΔG_t) for nano zinc ferrite prepared by sol–gel method at different mole fraction (Xs), different concentrations of CH_3·COOH at 318 K

Xs (CH_3·COOH)	S	Log S	log $\gamma_{\pm}$	pKsp	ΔG (J/mol)	ΔG_t (kJ/mol)
0.062	0.0071	− 2.1517	− 0.0425	2.1517	13,102.0441	0.0000
0.143	0.0084	− 2.0769	− 0.0463	2.0769	12,646.4330	− 0.4556
0.255	0.0102	− 1.9908	− 0.0512	1.9908	12,122.2116	− 0.9798
0.417	0.0129	− 1.8898	− 0.0575	1.8898	11,507.0003	− 1.5950

3.3.2 Solubility Product

The solubility product pKsp was calculated using Eq. (3) and the results obtained are listed in Tables 1, 2, 3, 4, 5, 6, 7, 8, 9, 10.

$$pKsp = -Log\ S \tag{3}$$

3.3.3 Activity Coefficient

The activity coefficients $\gamma_{\pm}$ were calculated using Debye–Hückel Eq. (4) [36] and the evaluated values are given in Tables 1, 2, 3, 4, 5, 6, 7, 8, 9, 10.

$$Log\gamma_{\pm} = -0.5062 \times (S)^{0.5} \tag{4}$$

Different methods are applied for the evaluation of the activity coeffiecients and all the used methods gave data little different from the other ones, like extended Debye–Hückel model using the known constants A and B explained in literature [36–38], and Davis model can be applied to nano zinc and nickel ferrites samples at 298 K with Davis constant A and the data obtained gave little different in activity coefficients, which affect very small the solubility parameters.The different methods for evaluation of the activity coeffiencts need a lot of data that not avialable. Then we suggested that no intermediate are formed. Therefore we applied the simple equation (Eq. 4) after Debye–Hückel.

3.3.4 Free Energy of Solvation

From the solubility products the Gibbs free energies of solvation and the transfer Gibbs free energies from water to mixed solvents were calculated by using (Eqs. 5 and 6). The computed data are also listed in Tables 1, 2, 3, 4, 5, 6, 7, 8, 9, 10 [35–39].

$$\Delta G = 2.303\ RT\ pKsp \tag{5}$$

$$\Delta G_t = \Delta G_S - \Delta G_w \tag{6}$$

3.3.5 Enthalpies and Entropies of Solvation

Using the solubility measurements at different temperatures and from the plots of log Ksp versus 1/T, the enthalpy (ΔH) values are calculated from the slope (slope = −ΔH/2.303R) [38–48]. Thus, the entropy (ΔS) of solvation for different nano nickel ferrite and nano zinc ferrite samples can be obtained using Gibbs–Helmholtz [48–52].

$$\Delta G = \Delta H - T\Delta S \tag{7}$$

The data obtained are given in Tables 11, 12.

3.3.6 Different Volumes of Nano Zinc Ferrite

The molar volumes (V_M) for $NiFe_2O_4$ and $ZnFe_2O_4$ nanoparticles were calculated from density measurements after subtracting the weight of 1 ml of saturated solutions from the empty weights of beakers. The V_M were obtained by dividing the molecular weight by the extract solution densities. The packing density (P) as explained in literature [41–46] is equal to the ratio of van der Waals volumes (V_W) to the molar volume (V_M) and equal to 0.664.

$$P = V_W/V_M = 0.664 \tag{8}$$

The data obtained are listed in Tables 13, 14, 15, 16, 17, 18, 19, 20, 21, 22.

The solubilities S, logS and pKsp for nano nickel ferrite at 298 K as shown in Table 1 are decreased with increase in acetic acid concentration favouring less nano salt–acid interaction. The Gibbs free energies are decreased also with

Table 11 Enthalpies and entropies of solubility parameters for nano nickel ferrite prepared by sol–gel method in different CH_3·COOH concentrations at different temperatures

Xs (CH_3·COOH)	ΔH (J/mol)	ΔS (298 K) (J/mol)	ΔS (303 K) (J/mol)	ΔS (308 K) (J/mol)	ΔS (313 K) (J/mol)	ΔS (318 K) (J/mol)
0.0620	24,992.2685	34.2212	34.1196	34.0828	34.3137	34.6114
0.1430	23,849.1192	32.9372	33.1579	32.8774	33.1052	33.3184
0.2550	22,772.9888	32.2474	32.3821	32.4618	32.2947	32.2058
0.4170	22,363.2167	34.1344	34.5786	34.6391	34.1862	33.8318

Table 12 Enthalpies and entropies of solubility parameters for nano zinc ferrite prepared by sol–gel method in different CH_3·COOH concentrations at different temperatures

Xs (CH_3·COOH)	ΔH (J/mol)	ΔS (298 K) (J/mol)	ΔS (303 K) (J/mol)	ΔS (308 K) (J/mol)	ΔS (313 K) (J/mol)	ΔS (318 K) (J/mol)
0.0620	28,754.8955	49.5136	49.7261	49.7532	49.5974	49.1996
0.1430	27,784.0803	48.0066	48.2405	48.2492	48.0932	47.5802
0.2550	27,322.6080	48.4625	48.6575	48.7632	48.5160	47.7775
0.4170	27,121.5516	49.7855	49.9748	50.1242	49.8240	49.0792

Table 13 Density (d), molar volume (V_M) and van der Waals volume (V_W) for nano nickel ferrite prepared by sol–gel method at different mole fraction (Xs), different concentrations of CH_3·COOH at 298 K

Xs (CH_3·COOH)	Molarity of CH_3·COOH	d (g/cm^3)	V_M (cm^3/mol)	V_W (cm^3/mol)
0.062	3	1.0093	232.2318	154.2019
0.143	6	1.0227	229.1818	152.1767
0.255	9	1.0370	226.0342	150.0867
0.417	12	1.0524	222.7210	147.8868

Table 14 Density (d), molar volume (V) and van der Waals volume (V_W) for nano nickel ferrite prepared by sol–gel method at different mole fraction (Xs), different concentrations of CH_3·COOH at 303 K

Xs (CH_3·COOH)	Molarity of CH_3·COOH	d (g/cm^3)	V_M (cm^3/mol)	V_W (cm^3/mol)
0.062	3	1.0184	230.1615	152.8272
0.143	6	1.0299	227.5943	151.1226
0.255	9	1.0446	224.3832	148.9904
0.417	12	1.0588	221.3748	146.9928

Table 15 Density (d), molar volume (V_M) and van der Waals volume (V_W) for nano nickel ferrite prepared by sol–gel method at different mole fraction (Xs), different concentrations of CH_3·COOH at 308 K

Xs (CH_3·COOH)	Molarity of CH_3·COOH	d (g/cm^3)	V_M (cm^3/mol)	V_W (cm^3/mol)
0.062	3	1.0292	227.7488	151.2252
0.143	6	1.0408	225.2064	149.5371
0.255	9	1.0536	222.4776	147.7251
0.417	12	1.0655	219.9827	146.0685

Table 16 Density (d), molar volume (V_M) and van der Waals volume (V_W) for nano nickel ferrite prepared by sol–gel method at different mole fraction (Xs), different concentrations of CH_3·COOH at 313 K

Xs (CH_3·COOH)	Molarity of CH_3·COOH	d (g/cm^3)	V_M (cm^3/mol)	V_W (cm^3/mol)
0.062	3	1.0373	225.9718	150.0453
0.143	6	1.0477	223.7149	148.5467
0.255	9	1.0591	221.3097	146.9496
0.417	12	1.0705	218.9630	145.3915

Table 17 Density (d), molar volume (V_M) and van der Waals volume (V_W) for nano nickel ferrite prepared by sol–gel method at different mole fraction (Xs), different concentration of CH3·COOH at 318 K

Xs (CH_3·COOH)	Molarity of CH_3·COOH	d (g/cm^3)	V_M (cm^3/mol)	V_W (cm^3/mol)
0.062	3	1.0479	223.6775	148.5218
0.143	6	1.0564	221.8851	147.3317
0.255	9	1.0647	220.1480	146.1783
0.417	12	1.0747	218.0919	144.8130

Table 18 Density (d), molar volume (V_M) and van der Waals volume (V_W) for nano zinc ferrite prepared by sol–gel method at different mole fraction (Xs), different concentrations of CH_3·COOH at 298 K

Xs (CH_3·COOH)	Molarity of CH_3·COOH	d (g/cm^3)	V_M (cm^3/mol)	V_W (cm^3/mol)
0.062	3	1.0359	232.7228	154.5280
0.143	6	1.0431	231.1059	153.4543
0.255	9	1.0524	229.0819	152.1104
0.417	12	1.0634	226.7045	150.5318

Table 19 Density (d), molar volume (V_M) and van der Waals volume (V_W) for nano zinc ferrite prepared by sol–gel method at different mole fraction (Xs), different concentrations of CH_3·COOH at 303 K

Xs (CH_3·COOH)	Molarity of CH_3·COOH	d (g/cm^3)	V_M (cm^3/mol)	V_W (cm^3/mol)
0.062	3	1.0411	231.5715	153.7635
0.143	6	1.0495	229.7016	152.5219
0.255	9	1.0595	227.5365	151.0842
0.417	12	1.0700	225.3062	149.6033

Table 20 Density (d), molar volume (V_M) and van der Waals volume (V_W) for nano zinc ferrite prepared by sol–gel method at different mole fraction (Xs), different concentrations of CH_3·COOH at 308 K

Xs (CH_3·COOH)	Molarity of CH_3·COOH	d (g/cm^3)	V_M (cm^3/mol)	V_W (cm^3/mol)
0.062	3	1.0456	230.5630	153.0938
0.143	6	1.0548	228.5488	151.7564
0.255	9	1.0647	226.4334	150.3517
0.417	12	1.0752	224.2165	148.8798

Table 21 Density (d), molar volume (V_M) and van der Waals volume (V_W) for nano zinc ferrite prepared by sol–gel method at different mole fraction (Xs), different concentrations of CH_3·COOH at 313 K

Xs (CH_3·COOH)	Molarity of CH_3·COOH	d (g/cm^3)	V_M (cm^3/mol)	V_W (cm^3/mol)
0.062	3	1.0497	229.6556	152.4913
0.143	6	1.0587	227.7073	151.1977
0.255	9	1.0678	225.7798	149.9178
0.417	12	1.0801	223.1896	148.1979

Table 22 Density (d), molar volume (V_M) and van der Waals volume (V_W) for nano zinc ferrite prepared by sol–gel method at different mole fraction (Xs), different concentrations of CH_3·COOH at 318 K

Xs (CH_3·COOH)	Molarity of CH_3·COOH	d (g/cm^3)	V_M (cm^3/mol)	V_W (cm^3/mol)
0.062	3	1.0546	228.6039	151.7930
0.143	6	1.0624	226.9179	150.6735
0.255	9	1.0720	224.8866	149.3247
0.417	12	1.0830	222.6053	147.8099

increase of the acid concentration proving the smaller interaction in case of increasing acid concentration.The transfer Gibbs free energies from 0.062 M to different acetic show more negative values by increase acid concentration supporting less solvation. log activity coefficients are decreased with rise of acetic acid concentration indicating less ion–ion interaction by the increase in acetic acid concentration.

The different thermodynamic parameters given in Tables 1, 2, 3, 4, 5 for the solvation of nano nickel ferrite in acetic acid solutions at different temperatures, 298, 303, 308, 313, 318 K, gave general trend in the decrease in all the given parameters indicating less solid acid interaction by the increase in temperature.

The Gibbs free energies given in Tables 1, 2, 3, 4, 5 are positive in their values indicating non spontaneous solvation reaction.

The nano zinc ferrite show smaller thermodynamic data for solvation of nano zinc ferrite than that of nano nickel ferrite indicating the less solubility of the former due to its satbility at all the used concentrations and temperatures. All Gibbs free energy values for nano zinc ferrite resulted from the solvation in acetic acid solutions are positive one indicating small spontaneous reactions. From Tables 6, 7, 8, 9, 10 for the thermodynamic parmeters for nano zinc ferrite in acetic acid solutions are dcreased by increase of temperature favoring less solid acid interaction. It is indicated from Tables 1, 2, 3, 4, 5, 6, 7, 8, 9, 10 that the Gibbs free energies of solvation for nano nickel ferrite are greater in positivity than nano zinc ferrite supporting more stability of nano nickel ferrite than nano zinc ferrite in solid–acetic acid solvation.

The thermal parameters enthalpies and entropies are represented in Table 11 for nano nickel ferrite at different temperatures and found to be entropic reaction,depend on entropy (positive values) and not enthalpaic reaction (endothermic positive values). Table 12 presented the thermal enthalpy and entropy values for the solvation of nano zinc ferrite in different concentrations of acetic acid. The enthalpies are positive values indicating endothermic reactions and are greater than that of nano nickel ferrite date given in Table 11 indicating more heat is needed for the dissolvation molar volumes solution of nano zinc ferrite. Entropies of solvation for nano zinc ferrite are greater than that of nano nickel ferrite can help in dissolution but the very big enthalpies and Gibbs free energies prevent the solvation process.

The densities given in Tables 13, 14, 15, 16, 17 for nano nickel ferrite in acetic acid solutions are increased with the increase in acid concentration and temperature indicating more solvation process. But the molar volumes (V_M) and van der Waals volumes (V_W) for nano nickel ferrite are decreased with the rise of acetic acid concentration and temperature due to the endothermic thermal enthalpies for this nano material. The solvation molar volumes

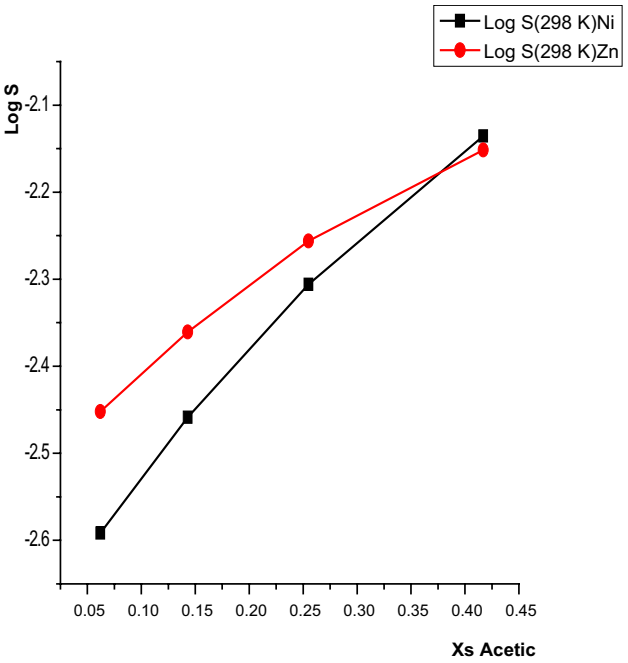

Fig. 3 Relation between (Log S) of nano nickel ferrite and nano zinc ferrite (sol–gel) and the mole fraction of CH_3·COOH at 298 K

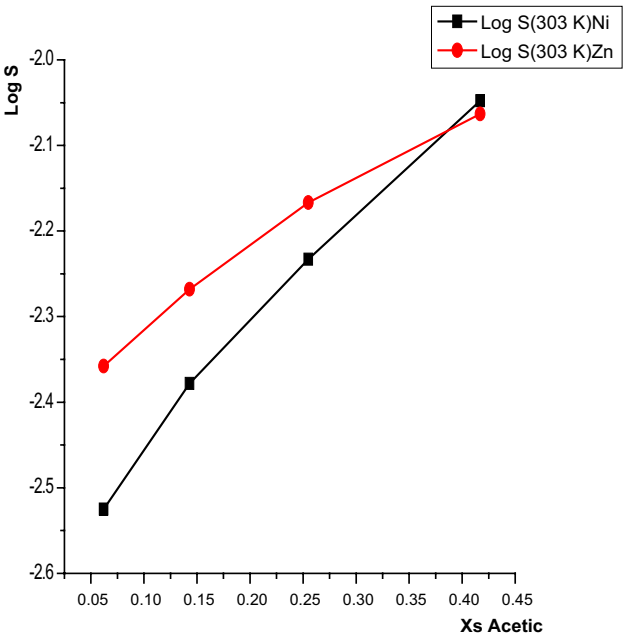

Fig. 4 Relation between (Log S) of nano nickel ferrite and nano zinc ferrite (sol–gel) and the mole fraction of CH_3·COOH at 303 K

and van der Waals volumes for nano zinc ferrite given in Tables 17, 18, 19, 20, 21, 22 are greater than that of nano nickel ferrite given in Tables 13, 14, 15, 16, 17 due to higher positive enthalpies of nano zinc ferrite than that of

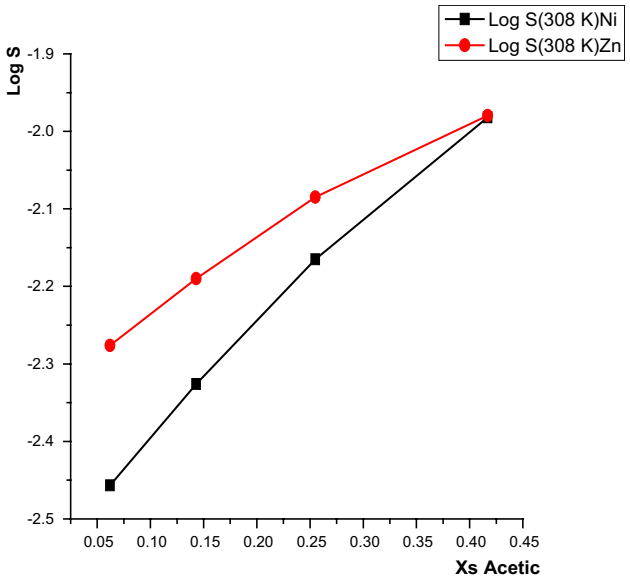

Fig. 5 Relation between (Log S) of nano nickel ferrite and nano zinc ferrite (sol–gel) and the mole fraction of CH_3·COOH at 308 K

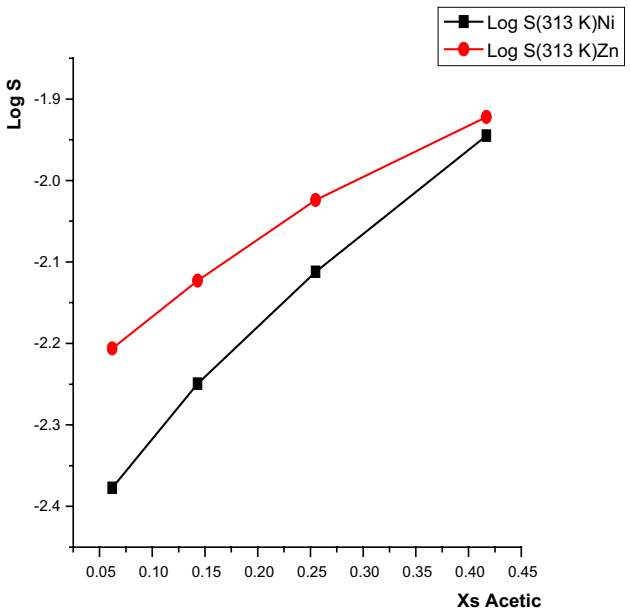

Fig. 6 Relation between (Log S) of nano nickel ferrite and nano zinc ferrite (sol–gel) and the mole fraction of CH_3·COOH at 313 K

nano nickel ferrite. The data given in Figs. 3, 4, 5, 6 and 7 show similar trend for both the solubilities of nano nickel ferrite and nano zinc ferrite at the different temperature studied. From these Figs. 3, 4, 5, 6 and 7 it is proved that the solubilities of nano nickel ferrite are greater than that of nano zinc ferrite.

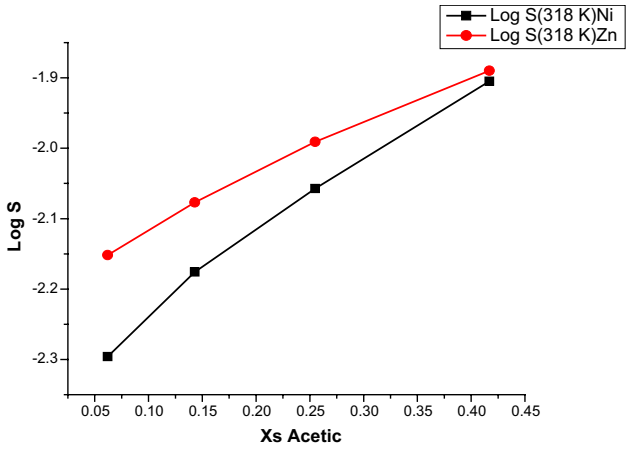

Fig. 7 Relation between (Log S) of nano nickel ferrite and nano zinc ferrite (sol–gel) and the mole fraction of CH_3COOH at 318 K

3.4 Theoretical Thermal Parameters

Quantum chemical calculations were done for nickel ferrite, zinc ferrite and nickel Zn ferrites were done to evaluate the theortical properties in aqueous media [48–52]. We use Hartee Fock method of calculating frequencies properties for the restricted orbitals, basis set 3-21G, using Gaussian 09 program. Nickel ferrite belongs big dipole moment, 13.64 (Debye), very high octopole moment 39 (Debye) and am greatest energy gap (0.27912 eV), difference between LUMO and HOMO orbitals). Zn ferrite show low dipole moment (7.5886 eV) and low energy gap (0.19185 eV).

Nickel zinc ferrite shows very high dipole moment (15.655 Debye) a medium energy gap (0.22425 eV). All the other thermal parameters,sum of electronic–thermal energies, zero point energies, sum of electronic–thermal enthalpies, sum of electronic–thermal free energies, heat capacity at constant volume CV, entropies S are given with lot properties in Appendix 1 (Online) explaining the improvment of the electrical, and thermal properties of zinc ferrite on adding nickel ferrite when mixing them in medicine to them and also decrease that for nickel ferrite indicating semiconductor properties of the mixture ferrites (most thermal properties are given in Hartree/particle).

4 Conclusion

The nano-sized nickel ferrite and zinc ferrite with spherical and cubic spinel crystal structure respectively (confirmed from XRD and TEM) were prepared using sol–gel method. The thermodynamic free energies of transfer (ΔG_t) for solvation for nano nickel ferrite in different concentrations of acetic acid increase in negativity with an increase of the mole fraction of acetic acid and their values are little affected

by temperature giving approximately similar data. The nano zinc ferrite shows similar Gibbs free energy data of solvation in different mole fractions of acetic acid at the used temperatures indicating little solvation. The enthalpies of solvation for nano nickel ferrite in acetic acid solutions are decreased in positivity with increase of acetic acid mole fraction in the used solutions. The reaction process not exothermic and is endothermic and depend on temperature and ΔG values. Nano zinc ferrite gave ΔH positive values and ΔS positive values indicating less spontaneous processes and endothermic behaviors in the used acetic acid solutions.

Compliance with Ethical Standards

Conflict of interest The authors declare that they have no conflict of interest.

References

1. M. Khairy, Ph.D. Thesis, Benha University, Egypt (2008)
2. H. Grabowska, W. Mis, J. Trawczyn, J. Wrzyszcz, M. Zawadzki, Res. Chem. Intermed. **27**(3), 305–313 (2001)
3. D.S. Kumar, K.C. Mouli, Int. J. Nanotechnol. Appl. **4**, 51–59 (2010)
4. M. Zayat, D. Levy, Chem. Mater. **12**, 2763–2769 (2000)
5. K. Okuyama, I.W. Lenggoro, Chem. Eng. Sci. **58**, 537–547 (2003)
6. Y. Marcus, Pure Appl. Chem. **62**, 2167–2219 (1990)
7. M. Rivero, A. del Campo, Á. Mayoral, E. Mazario, Jorge Sánchez Marcos Alexandra Muñoz-Bonilla. RSC Adv. **6**, 40067–40076 (2016)
8. O.M. Lemine, M. Bououdina, M. Sajieddin, A.M. Al-Saie, M. Sha, A. Khatab, M. Al-hilal, Henini. Physica B **406**, 1989–1994 (2011)
9. L.W. Yeary, J.W. Moon, C.J. Rawn, L.J. Love, A.J. Rondinone, J.R. Thompson, B.C. Chakoumakos, T.J. Phelps, J. Magn. Magn. Mater. **323**(23), 3043–3048 (2011)
10. C. Xiangfeng, J. Dongli, Z. Chenmou, Sens. Actuator B **123**, 793–797 (2007)
11. S.L. Darshane, S.S. Suryavanshi, I.S. Mulla, Ceram. Int. **35**(2009), 1793–1797 (2009)
12. B.M. Berkovsky, V.F. Medvedev, M.S. Krakov, *Magnetic Fluids: Engineering Applications*, 1st edn. (Oxford University Press, Oxford, 1993)
13. M.M. Rashad, O.A. Fouad, Mater. Chem. Phys. **94**, 365–370 (2005)
14. S. Rana, R.S. Srivastava, M.M. Sorensson, R.D.K. Misra, Mater. Sci. Eng. **119**(2), 144–151 (2005)
15. M. Kulkarni, U.V. Desai, K.S. Pandit, M.A. Kulkarni, P.P. Wadgaonkar, RSC Adv. **4**, 36702–36707 (2014)
16. S. Mukherjee, M.K. Mitra, Adv. Mater. Lett. **6**, 902–906 (2015)
17. V. Sunny, P. Kurian, P. Mohanan, P.A. Joy, M.R. Anantharaman, J. Alloys Compd. **489**, 297–303 (2010)
18. G. Fan, Z. Gu, L. Yang, F. Li, Chem. Eng. J. **155**, 534–541 (2009)
19. Z. Jia, D. Ren, Y. Liang, R. Zhu, Mater. Lett. **65**, 3116–3119 (2011)
20. X. Li, Y. Hou, Q. Zhao, G. Chen, Langmuir **27**, 3113–3120 (2011)
21. K.J. McDonald, K.S. Choi, Chem. Mater. **23**, 4863–4869 (2011)
22. G. Lu, S. Li, Hydrog. Energy **17**, 767–770 (1992)
23. H. Lv, L. Ma, P. Zeng, D. Ke, T. Peng, J. Mater. Chem. **20**, 3665–3672 (2010)
24. T. Liu, L. Wang, P. Yang, B. Hu, Mater. Lett. **62**(24), 4056–4058 (2008)
25. S. Abou Elleef, E. Gomaa, Int. J. Eng. Innov. Technol. **3**, 308–313 (2013)
26. E.A. Gomaa, Am. J. Syst. Sci. **3**, 12–17 (2014)
27. A.A. El Khouly, E.A. Gomaa, S.M. Abou Elleef, Bull. Electrochem. **19**(4), 153–164 (2003)
28. H. Kavas, N. Kasapoglu, A. Baykal, Y. Koseoglu, Chem. Pap. **63**, 450–455 (2009)
29. S.K. Milonjic, J. Serb. Chem. Soc. **72**(2), 1363–1367 (2007)
30. E.A. Gomaa, M.H. Mahmoud, M.G. Mousa, E.M. El-Dahshan, Chem. Methodol. **3**, 1–11 (2018)
31. T. Tripathi, J. Proteins Proteomics **4**(2), 85–91 (2013)
32. E.A. Gomaa, R.M. Abu-Qarn, J. Mol. Liq. **232**, 319–324 (2017)
33. E.A. Gomaa, R.R. Zaky, A. Shokr, J. Mol. Liq. **241**, 913–918 (2017)
34. E.A. Gomaa, M.A. Tahoon, A. Negm, J. Mol. Liq. **24**, 595–602 (2017)
35. N. Erfaninia, R. Tayebee, E.L. Foletto, M.M. Amini, M. Dusek, F.M. Zonoz, Appl. Organomet. Chem. **32**, 1–7 (2017)
36. S.L. Oswal, J.S. Desai, S.P. Ijardar, D.M. Jain, J. Mol. Liq. **144**, 108–114 (2009)
37. E.A. Gomaa, Croat. Chem. Acta **62**(3), 475–480 (1989)
38. J.I. Kim, A.H. Cecal, J. Born, E.A. Gomaa, Z. Phys. Chem. **110**, 209 (1978)
39. C.W. Davis, *Ion Association* (Butter Worth, London, 1962)
40. D. Bobicz, W. Grzybkowski, A. Lwandowski, J. Mol. Liq. **105**(93), 99–227 (2003)
41. Y. Marcus, *The Properties of Solvents* (Wiley, Chichester, 1998)
42. E.A. Gomaa, A.H. El-Askalany, M.N.H. Moussa, Asian J. Chem. **4**, 553–558 (1992)
43. O. Popvych, A. Gibofsky, D.H. Berne, Anal. Chem. **44**(4), 811–817 (1972)
44. M. Isabel, L. Lampreia, A. Ferreira, J. Chem. Soc. Faraday Trans. I **92**, 1487 (1996)
45. P.W. Atkins, *Physical Chemistry* (Oxford University Press, Oxford, 1978)
46. D. Ives, *Chemical Thermodynamics* (Macdonald Technical and Scientific, London, 1971)
47. Esam A. Gomaa, Phys. Chem. Liq. **50**, 279–283 (2012)
48. E.A. Gomaa, M.A. Mousa, A.A. El-Khouly, Thermochim. Acta **86**, 351–356 (1985)
49. E.A. Gomaa, M.A. Mousa, A.A. El-Khouly, Thermochim. Acta **89**, 133–139 (1985)
50. Elsayed M. AbouElleef, Esam A. Gomaa, Mai S. Mashaly, J. Biochem. Tech. **9**(2), 42–47 (2018)
51. M.A. Tahoon, E.A. Gomaa, M.H.A. Sulelman, Open. Chem. **17**, 260–269 (2019)
52. H. Zarrok, S.S. Al-Deyab, A. Zarrouk, R. Salghi, B. Hammouti, H. Oudda, M. Bouachrine, F. Bentiss, Int. J. Electrochem. Sci. **7**, 4047–4063 (2012)